Solvation properties of the actinide ion Th(IV) in DMSO and DMSO:water mixtures through polarizable molecular dynamics

Maria Montagna,[†,¶] Riccardo Spezia,[‡] and Enrico Bodo[*,†]

†*Chemistry Department, University of Rome "La Sapienza", P. A. Moro 5, 00185, Rome, Italy*

‡*LAMBE, Université d'Evry Val d'Essonne, CEA, CNRS, Université Paris Saclay, F-91025 Evry, France*

¶*Present Address: Leibniz Institute of Polymer Research Dresden, Dresden, Germany*

E-mail: enrico.bodo@uniroma1.it

Abstract

We have studied the solvation of Th^{4+} in water, dimethylsulfoxide (DMSO) and in their equimolar mixture by using molecular dynamics based on a Amoeba-derived polarizable force field. We have performed an extended structural analysis in order to provide a complete picture of the chemical-physical features of the interaction of Th^{4+} with the two solvents either in their pure and mixed states. Through our simulations we found that, very likely, the first solvation shell in DMSO is not unlike the one found in pure water and contains 9 solvent molecules. The residence time of first shell of DMSO molecules is however much longer than the residence time of water. For the 1:1 mixture we present computational evidence that both water and DMSO participate to the solvation of Th^{4+} with a slight preference for the latter.

Introduction

The study of the solvation processes of actinoids (An) in organic solvents represents a fundamental step for the design of separation and recovery processes of these very expensive elements. In particular, for actinoids, one of the most important industrial process involving these heavy elements is their separation from nuclear waste, a task which is generally performed by using organic solvents to extract the ions from the aqueous phases with different techniques and operating conditions.[1–6] It therefore follows that the possibility of providing unambiguous answers to the many questions raised by this technological challenge using *in silico* simulations is of great advantage especially because it reduces the need of experimental assessments that involve the use of highly poisonous/radioactive substances. While for hydration of actinoids, a relatively high number of experimental and theoretical studies have been reported in the literature,[7–34] much less is known for other oxygen donors organic solvents such as DMSO.[35] The very few studies reported are on uranyl in DMSO[36,37] and other solvents[38,39] while for bare ions only a small number of crystal structures are available.[40–45] Th^{4+} in liquid DMSO and N,N- dimethylpropyleneurea (DMPU) was studied experimentally

by Torapava et al.[35] using X-ray absorption fine structure (EXAFS) technique.

Actinoid ions show different oxidation states depending on their position along the series and on the chemical environment: all heavy ions (from Am to Lr) have oxydation state III, while for the light ones the situation is more complex with oxidation states ranging between II and VI .[46] Oxydation state IV, in particular, is typical of bare cations of light actinoids, and it turns out to be the most stable state for Th, but it has also been observed for Pa, U, Np and Pu. Some of these ions were studied as bare cations in water by both experiments and theory.[8,9,12,14,18,19,22,23,28,30,33] Among them Th^{4+} is probably the most studied one, because it is easier to handle from an experimental point of view (it is stable and not dangerous) and, theoretically, it is the less problematic to treat since it is a closed shell species. It was indeed recently shown that a single determinant representation is well suited when treating Th^{4+}.[30]

We focus our attention on the solvation of Th^{4+} since it represents a good model to understand dissolution of light bare actinoid cations in oxygen donor solvents, a choice which is further motivated by the fact that information on its coordination in two oxygen donor solvents (di-methyl-sulfoxyde (DMSO) and di-methyl-propyl-urea (DMPU)) has recently become available.[35,47]

Recently, we have shown that the use of an approach based on the study of small clusters of solvent molecules is extremely useful and we have used it to gather information on the DMSO structure around highly charged ions.[47,48] The great advantage of this approach is that it is possible to make use of accurate quantum chemistry methods, not only to obtain the possible coordination geometries, but also to extract and test a specific model for the interaction of these highly charged ions that can be integrated into a polarizable force field such as Amoeba.[49] Here, we have used the results obtained by us on Th^{4+}@DMSO clusters[47] to develop a simple, transferable, polarizable force field able to describe the solvation of the ion in different solvents. We will therefore present a test case study for water solvation (that is needed to check the trasferability of the force field), a new set of calculations for solvation

of Th^{4+} in pure liquid DMSO and in a water/DMSO 1:1 mixture.

Methods

Force Field Development

Molecular dynamics simulations have been performed using the *Tinker*[50] package with a modified *Amoeba*[49] force field. The parameters for water and DMSO are those of the Amoeba[49] force field with small modifcations for the latter.[51] The Th^{4+}-DMSO/water interactions are not available in the Amoeba force field and we supply here new parameters for it. To this end we have kept fixed DMSO parameters and adjusted the Th^{4+} ones. The ion is described by its polarizability that has been set to 1.143 $Å^3$ (taken from the ab-initio calculations of ref.[52]), and by its van der Waals parameters that have been generated by using a "trial and error" procedure that consists in comparing the structures and the energies of the ab-initio minimum geometries of clusters with a high number of DMSO molecules[47] with the corresponding structures obtained using the force field. In particular we have used the structures containing 8 and 9 DMSO molecules,[47] optimized at the M06-2X/6-31G* level in which the small core ECP and the ECP60MWB basis (whose contraction is (12s, 11p, 10d, 8f) $\rightarrow$ [8s, 7p, 6d, 4f]) was used for Th^{4+}.[53]

The results in terms of Th-O distances and interaction energies are reported in Table 1 where we can see that the force field is able to grasp both the energetic (with errors well within 10%) and the shape of the ab-initio optimized structures (with errors of few hundredths of Å). In the same table we also report a comparison between our modified Amoeba force field and MP2 results of Marjolin et al.[23] in terms of geometrical parameters and energetic of Th^4-water clusters. The good agreement provides a measure of the transferability of the van der Waals parameters (here parametrized on Th^{4+}:DMSO cluster) to the Th^{4+}-water interaction.

The final values for the van der Waals Th^{4+} parameters that we have used are σ=4.04

Å and ϵ=3.4 kcal/mol. This set of parameters turned out to be not very different from the one published in ref.[23] parametrized for Th^{4+}-water solvation and where, however, the final Th-O distances in water resulted to be slightly underestimated with respect to experimental values. For further details on the force field derivation see the Supporting Information (Section S1).

In order to further ensure that our new model potential was able to reproduce the behavior of the the Th^{4+}-O interaction we have performed a constant temperature (with T=100 K) molecular dynamics simulation on the isolated $[Th(DMSO)_9]^{4+}$ cluster. The simulation was carried out for 500 ps (using the same simulation set-up described in next section). The power spectrum (vibrational density of states) was then extracted using the velocity autocorrelation function. The final power spectrum was then compared with the vibrational frequencies as obtained by the ab-initio DFT minimization mentioned before. In the classical simulation the Th^{4+} ion is seen to contribute to the vibrational density of states only at low frequencies and its main contributions are localized below 300 cm^{-1}. The frequencies of these bands are in decent agreement with those obtained by the ab-initio normal modes analysis thereby providing evidence for the accuracy of the present force field in describing the overall interactions, at least, in the first solvation shell. More details on this computational experiment can be found in the Supporting Information (Section S2 and Figure S1).

Table 1: Geometric parameters and interaction energies for Th^{4+}@DMSO clusters with different computational methods. The data from ref.[23] are at the MP2 level. The numbers in parenthesis are the percentage energy difference of the Amoeba FF with the ab-initio value reported on the previous row.

Method	Th-O distance (Å)		Int. Energy (kcal/mol)	
	$[Th(DMSO)_8]^{4+}$	$[Th(DMSO)_9]^{4+}$	$[Th(DMSO)_8]^{4+}$	$[Th(DMSO)_9]^{4+}$
M062x	2.42	2.47	-1181.8	-1227.2
B3LYP	2.43	2.49	-1180.9	-1219.5
Amoeba	2.42	2.47	-1097.7 (ΔE=7%)	-1116.4(ΔE=8%)
	$[Th(H_2O)_8]^{4+}$	$[Th(H_2O)_9]^{4+}$	$[Th(H_2O)_8]^{4+}$	$[Th(H_2O)_9]^{4+}$
Ref[23]	-	2.4	-740.04	-786.56
Amoeba	2.48	2.51	-708.0 (ΔE=4%)	-744.6(ΔE=5%)

Molecular Dynamics

Molecular dynamics simulations have been performed on three systems made by a single Th^{4+} ion surrounded respectively by (i) 267 water molecules, (ii) 68 DMSO molecules and (iii) an equimolar water/DMSO mixture made by 50 water molecules and 50 DMSO molecules. Each system has been equilibrated using the NPT ensemble (with a Berendsen barostat[54]) at room conditions for 2 ns while the production was carried out in the NVT ensemble (with a Berendsen thermostat[54]) and lasted about 15 ns. The timestep was set to 1 fs and the system coordinates and velocities have been saved each 100 fs. The regular Ewald method has been used for the electrostatic energy calculation with a cutoff of 9 Å. No constraints have been used. These timescales should allow us to grasp the relatively long residence times of the solvents molecules around such highly charged specie. To verify that simulations are equilibrated we have followed the time evolution of the Mean Square Displacements (MSD), which reaches a linear regime for both solvents, also in the case of the mixture (Section S3 in the Supporting Information, and in particular Figure S2).

After equilibration, the density of the cells obtained by subtracting the Th mass, is 0.994 gr/cm^3 for pure water, 1.073 gr/cm^3 for pure DMSO and 1.063 gr/cm^3 for the 1:1 mixture. These numbers are in good agreement (within 2%) with well known density data and those reported in ref.[55] for the mixture. The performance of the force field in predicting the density of the liquid surrounding the ion at room conditions is remarkably good (considering also the marginal, but sizable "electrostriction" effect due to the increased density of the solvent around the ion). As a further test of the potential we have calculated the self-diffusion coefficient of the Th^{4+} ion in pure water ($1.7 \cdot 10^{-10} \pm 0.7$ m^2/s) and compared it to the experimental value reported in ref.[56] ($1.53 \cdot 10^{-10}$ m^2/s). Despite our force field overestimate the diffusion coefficient the error is acceptable for such quantity and is largely inside the uncertainties. Therefore, we can be confident that the potential model will be able to describe structure and dynamics of such systems.

Results and Discussion

Structural Properties

We report in Figure 1 the Radial Distribution Functions (RDFs) for the Th-O distances in the solution with pure water (left), pure DMSO (center) and the 1:1 solution (right) along with their volumetric running integral (i.e. the coordination number (CN)). The average distance from our calculations are compared with available data from recent experiments in Table 2. The distances presented in Table 2 show the very good performance of the force field in grasping the first shell structure around the central ion with respect to experiments and simulations.

A Benchmark System: Th^{4+} in H_2O

We now discuss the performances of the model in describing Th^{4+} hydration. An important point is that, although the model potential has been developed using the $[Th(DMSO)_n]^{4+}$ clusters, it performs quite well in predicting also the structure of Th^{4+} in liquid water thereby showing its transferability to other systems. We have first to notice that average Th-O(water) distances reported in Table **??** are in agreement with both EXAFS[8,18] and HEXS[16] experiments, even if the distances in the cluster slightly overestimate the Th-O distance with respect to MP2 calculations (see Table 1). The Th-O distances in our simulations are similar to those coming from the previously developed Amoeba force-field (see Table 2), although, given that our CN turns out to be 9.2, a 10-fold coordinated structure must, necessarily, exist in our simulations, while the previous force field reports only the presence of a 9-fold structure.[23] Other simulations show similar distances[19,22] to ours, while some[9,28] report distances that are larger than ours of about 0.1 Å.

Within our simulations, a non-integer CN (9.2) has been obtained and this indicates a dynamical interconversion between 9- and 10-fold coordinated structures in water solution. This is a frequent situation for such heavy ions and as been already noticed for lanthanoid(III)

ions in water,[57,58] in DMSO[51] and actinoid(III) ions in water.[21] The coexistence of different solvation patterns might also explain the dispersion of the experimental values of the CN values that is present in the literature. In fact, some experiments[8,16] report CN=10 while others[18] CN=9. Simulations have often reported that the 9-fold structure is dominant (or even the only possible one).[9,23,28,59] Real et al.[19] obtained a CN of 8 and showed that a cohexistence between CN=8 and CN=9 can be obtained by varying slightly the force field parameters.[19] Recent simulations using the polarizable NEMO force field reported a CN of 9.5 that, as in our case, stems from the coexistence of 9- and 10-fold structures.[22] Furthermore, DFT-based free energy calculations[22] reported that the coordination motif with CN=9 is more stable than the one with CN=10 by about 3 kcal/mol or 1 kcal/mol depending on the functional employed, thereby proving the dominant contribution of CN=9 in pure water. Note that experimental data depends also on the concentration, in particular when Cl^- is used (while it is less concentration-dependent in the case of Br^-, see Ref.[16]). Given that, in the present study, the Th^{4+} hydration mainly serves as a benchmark of the force field and to evaluate its transferability, the best possible comparison is with calculations done in the ideal conditions of infinite dilution. Furthermore, we should note that in the interpretation of EXAFS measurements, the CNs depend on the fitting procedure and it is well known that the associated uncertainty is of the order of $\pm$ 0.5. Therefore the value that we have obtained here (9.2) fits well with the experimental determinations of CN = 9. We also note that EXAFS based measurements often assume an integer coordination number even when inter-shell exchange dynamics occurs. As it has been pointed out in several lanthanoid(III) and actinoid(III) ions hydration studies, taking into account the dynamical exchange picture as highlighted by simulations, it has been possible to reduce the EXAFS CN uncertainty and to provide an almost perfect agreement between experiments and simulations. In this way, some previous integer CNs reported have been revised[27,60] and the dynamical exchange picture of solvation in liquid phase is now the generally accepted one.[7] Note also that, for lanthanoid(III) ions, these results were in agreement with the self-exchange mechanisms of

water molecules in the first shell of solvation ions, as reported by Helm and Merbach.[61] In the case of Th^{4+} hydration, unfortunately, there are no experimental data on such self-exchange kinetics.

Finally, only very few experimental data are reported for the second shell of solvation. Our results provide a position of the second peak of the RDF at around 4.5 Å which agrees well with the experimental data of 4.657 Å proposed by Torapava et al..[18]

We conclude this section, by noticing that, we reported the hydration properties of Th^{4+} as a mean to prove that our force field parameters, that have been fitted on Th^{4+}:DMSO clusters, are, nevertheless, transferable also to water. The hydration properties, which have been largely studied in the recent past, provides us with a perfect benchmark system. The good agreement between our results and previous studies gives us confidence in the reliability and transferability of the force field.

Th^{4+} in pure DMSO

We now move to the description of the simulation data for Th^{4+} in pure DMSO. Structural data as obtained by our simulations are compared with the experimental ones in Table 2 while the Th^{4+}-O RDF is reported in Figure 1 (middle panel). The first solvation shell of oxygen atoms is correctly predicted to lie between 2.4 and 2.6 Å in agreement with the only available experimental data.[35] The second shell appears to lie between 6 and 8 Å and turns out to be less structured when compared to the water case because of the much larger distance of the second shell DMSO molecules from the coordinating cation and the consequently reduced electrostatic interaction between them and the central ion. Concerning the coordination number, our force field predicts a value of 9 for the DMSO solvation which is also in agreement with the data reported experimentally.[35] The first-shell Th-S average distance is overestimated by about 0.2 Å with respect to experiments.[35] This discrepancy is due to the inability of the present force field to reproduce correctly the $Th\cdots O{-}S$ angle. Despite our efforts in the optimization process of the potential, the force field predicts a coordination

pattern where the S=O bond lies in line with the O-Th direction. The $Th^{4+}@(DMSO)_n$ cluster ab-initio calculations,[47] on the other side, predicts a bent geometry for the Th$\cdots$O$-$S binding pattern. This problem is probably due to the simplified (electrostatic) potential model inherent to the force field approach that, very likely, does not take into account the electronic delocalization effects along the Th$\cdots$O$-$S binding motifs that may promote a bent geometry of the complex.

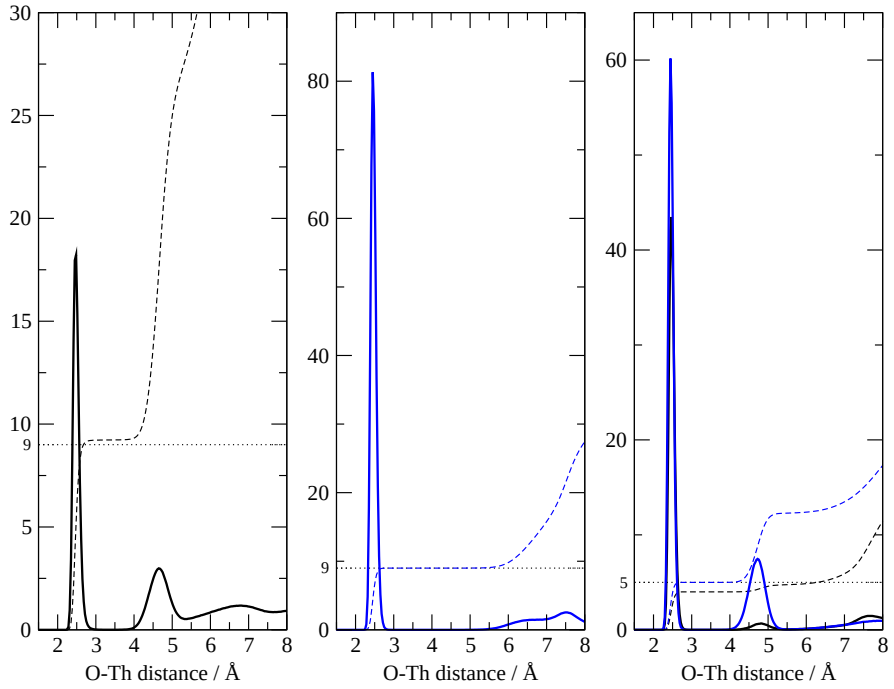

Figure 1: Th-O RDF and coordination numbers for Th^{4+} in pure water (left), pure DMSO (middle) and 1:1 water DMSO mixture (right) solutions according to our simulations. Water: black line, DMSO: blue line.

A visual representation of the geometry of the first shell in pure DMSO can be obtained from the density of the atomic positions of the coordinating molecules averaged over 5 ns of trajectory. This is shown in Figure 2. On the left we can see the "geometry" of the first shell of the 9 coordinating oxygen atoms. This shell is rather rigid but the internal conformational mobility makes the global shape to either that of a tricapped trigonal prism or a monocapped square antiprism. On the right side of Figure 2 we report together with the oxygen density

Table 2: Structural data as obtained from our simulations as compared with previous experiments and simulations. EXAFS = extended X-ray fine structure; HEXS = high-energy X-ray source; MD = molecular dynamics; QMCF = quantum mechanical charge field; DFT = density functional theory; POL = polarizable; CL = classical; NEMO and Amoeba refer to the named force fields.

System	Method	r_{Th-O} (Å)	$CN^{(1)}$	r_{Th-S} (Å)	Reference
Th^{4+} in H_2O					
	Amoeba-MD	**2.465**	**9.2**		This work
	Amoeba-MD	2.40	9		Ref.[23]
	QMCF-MD	2.54	9		Ref.[28]
	DFT-MD	2.50	9		Ref.[59]
	DFT-MD	2.46/2.49	8/9		Ref.[22]
	POL-MD	2.45	9		Ref.[22]
	NEMO-MD	2.45	9.5		Ref.[22]
	CL-MD	2.44/2.47	8.05/8.45		Ref.[19]
	CL-MD	2.54	9		Ref.[9]
	EXAFS	2.45	10		Ref.[8]
	EXAFS	2.45	9		Ref.[18]
	HEXS	2.46	10		Ref.[16]
Th^{4+} in DMSO					
	Amoeba-MD	**2.455**	**9**	**3.955**	This work
	EXAFS	2.447	9	3.672	Ref.[35]
Th^{4+} in H_2O/DMSO (1:1)					
DMSO:	Amoeba-MD	**2.451**	**5**	**3.945**	This work
H_2O:	Amoeba-MD	**2.463**	**4**		This work

(in red) also the average position of the sulfur atoms (yellow) and of the carbon atoms (gray, transparent color). Similarly to the oxygen atoms, the sulfur atoms are quite localized in space even though their angular mobility is larger than that of the oxygen. The carbon atoms density is instead highly delocalized and give rise to a substantially uniform density sphere surrounding the internal cavity. The conformational freedom of the carbon atoms is due to the dynamical rotation of the DMSO molecule around the S=O axis.

Another way of looking at the conformational mobility of the solvation shell is reported in Figure 3 where we have calculated for the 9 molecules of the solvation shell the combined angular-radial distribution function. The first features on the left, at short range, are the oxygen atoms localized at around 2.5 Å and with a bimodal angular distribution in the $O\hat{T}hO$ angle. The first peak at 65° is due to adjacent atoms on an edge of the polyhedra while the second peak at 140° is due to the atoms that are 2 edges far from each other. As we can see the same polyhedric structure is preserved when moving from the oxygen to the sulfur that merely presents the same angular pattern at a larger distance of about 4 Å. A totally different angular map is instead shown by the carbon atoms which have an unstructured angular distribution and a much broader radial distribution. In this case, the feature around 30° that we see at the bottom of the plot is due to the almost fixed $C\hat{T}hC$ angle when the carbon atoms are part of the same molecule. We conclude that, despite the almost rigid structure of the first shell, the DMSO solvation presents an additional source of disorder due to the flexibility of the methyl chains around the solvated ion.

Th^{4+} in a 1:1 mixture H_2O/DMSO

We now move to the Th^{4+} in a 1:1 mixed solution of H_2O and DMSO, for which the Th^{4+}-O RDF is shown in Figure 1 (right panel). We should note that the oxygen atoms of H_2O and DMSO are very close in distances, as detailed in Table 2. Total coordination number is still 9 which results from 5 DMSO and 4 H_2O molecules. This mixed solvation clearly stems from the fact that the main contribution to the total interaction of the first solvation shell comes

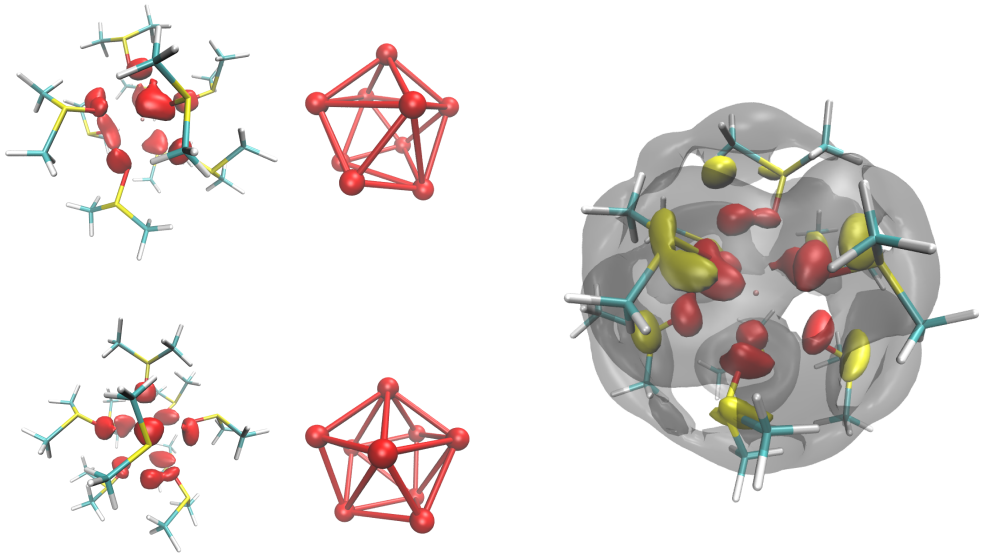

Figure 2: Left (above and below): density map of the average positions of the oxygen atoms in the first shell from two different points of view to highlight either the trigonal shape (below) or the square antiprims one (above). A ball-and-stick representation has also been added to help the identification of the structures. Right: density map of the oxygen (red), sulphur (yellow) and carbon (transparent gray) atoms around the Th ion. Each iso-surface has been chosen in order to include 10% of the total density of the atoms.

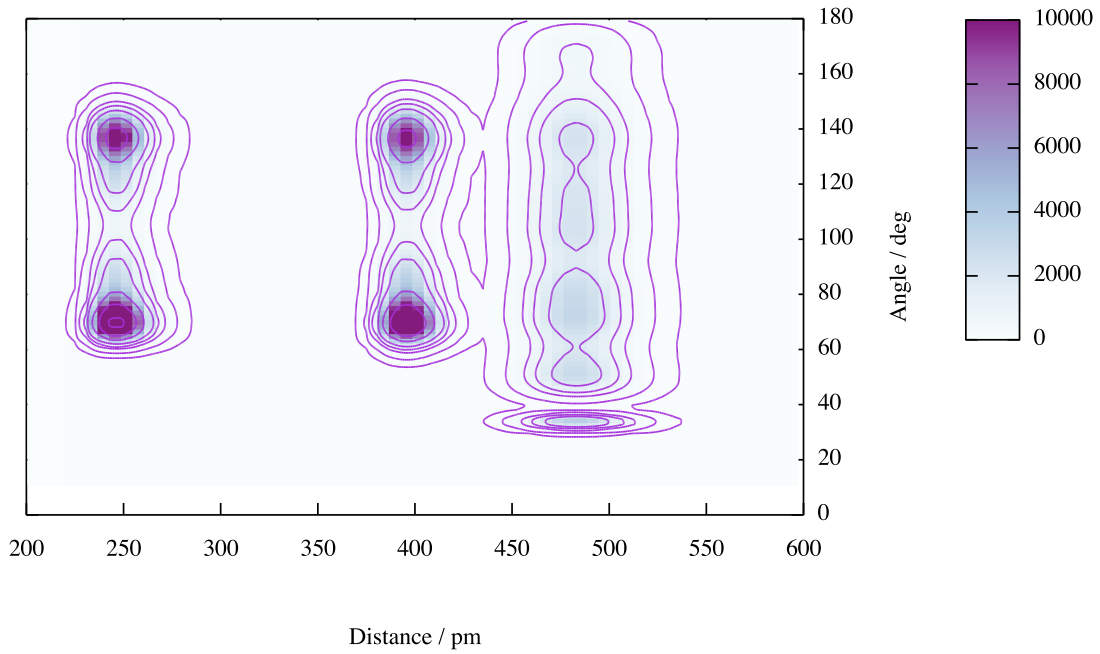

Figure 3: Combined angular-radial distribution function for the Th-DMSO distances. The first group on the left is the Th-O distance, far on the right there are the Th-C distances and in the middle the Th-S ones. The angle on the y-axis is between the two atoms and centered on Th. The contours are drawn at 8 values of the function from 10 to 20000.

from electrostatic energy and the two oxygen donor solvents behave in a quite similar way from the electrostatic point of view.

To compare the pure solvents solvation with that reported for the 1:1 solution, we show in Figure 4, on an expanded scale, the RDF for the Th-O distance. Few interesting remarks can be highlighted from this comparison:

1. The water molecules in the first shell essentially have the same Th-O distance both in the pure and in the 1:1 solution.

2. The second shell of water molecules that can be seen in the pure water simulation almost disappears when mixed with DMSO.

3. The Th-O average distance in the 1:1 mixture (2.451 Å) is slightly shorter than in pure DMSO (2.455 Å). See also the inset in Figure 4. The effect is, however, very small and within the statistical uncertainty of ±0.15 Å, computed as the average standard deviation (square root of the sum of variances) associated with the Th-O distances of the 5 DMSO molecules.

4. The DMSO in the 1:1 mixture shows a well defined second shell of DMSO molecules at 4.7 Å that is completely absent in the pure DMSO case.

The above features of the first solvation shell in the 1:1 mixture are mainly due to the different molecular sizes of the solvents involved: in particular the diminished steric hindrance of the water molecules is at the origin of the second shell peak on the RDF of Th-DMSO: the reduced molecular volume of the 4 coordinated water molecules allows for roughly 6 additional DMSO molecules to bring themselves near the central ion albeit remaining in the second shell of solvation.

An analysis of the density of the atomic positions for the first shell is reported in Figure 5 where we plot the total density of oxygen atoms in the first shell (cyan, transparent) and its decomposition into water (red) and DMSO (blue) molecules. As we can see, the geometry of

the first shell is much less structured than that of the pure DMSO case above. It turns out impossible to match a clear geometric structure on it, although it is still possible to discern a trigonal symmetry. While the density of oxygen atoms from the DMSO molecules is quite localized in space, the water one is broadly delocalized.

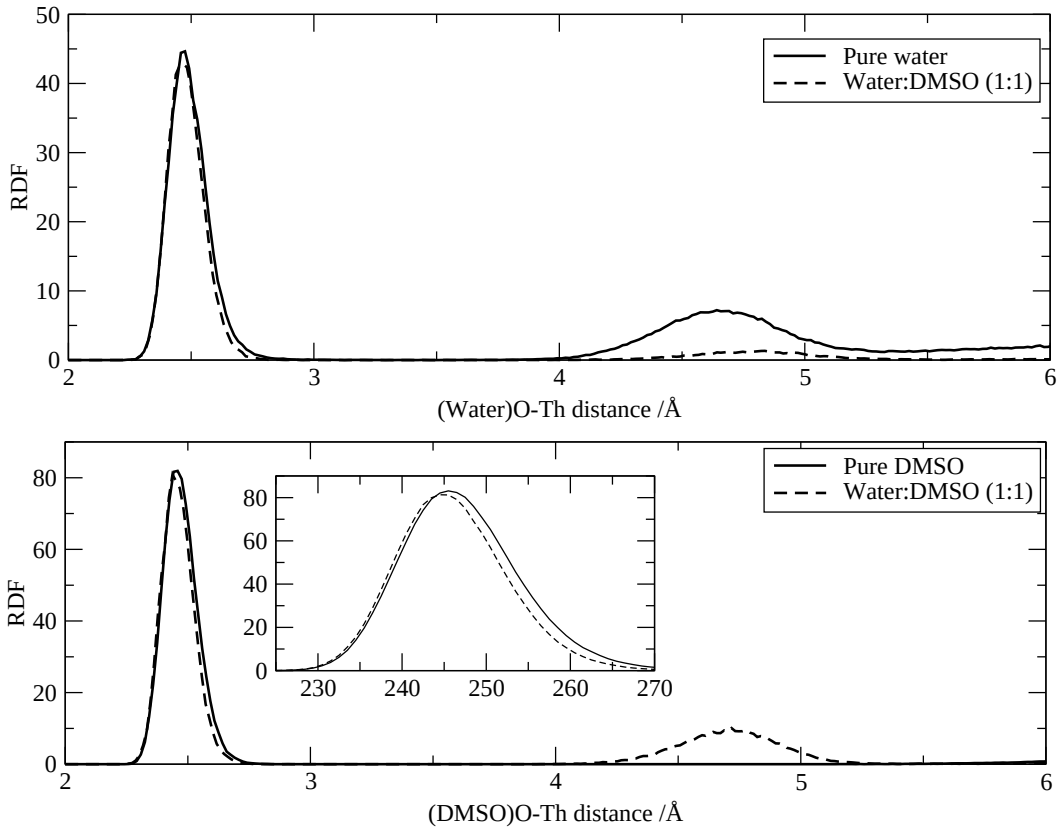

Figure 4: Th-O RDF for Th^{4+} in water (pure and mixture, upper panel) and DMSO (pure and mixture, lower panel).

Solvation Dynamics

As we pointed out above, the water molecules are much more mobile than the DMSO ones which, in turn, are more strongly bound to the central ion owing to their larger dipole moment (force field values are 4.235 D for DMSO and 1.77 D for water). In order to establish the dynamics at play in the first solvation shell we have collected in Figure 6 the Th-O distances as a function of time for an appreciable portion (10 ns) of the trajectory. In the two panels

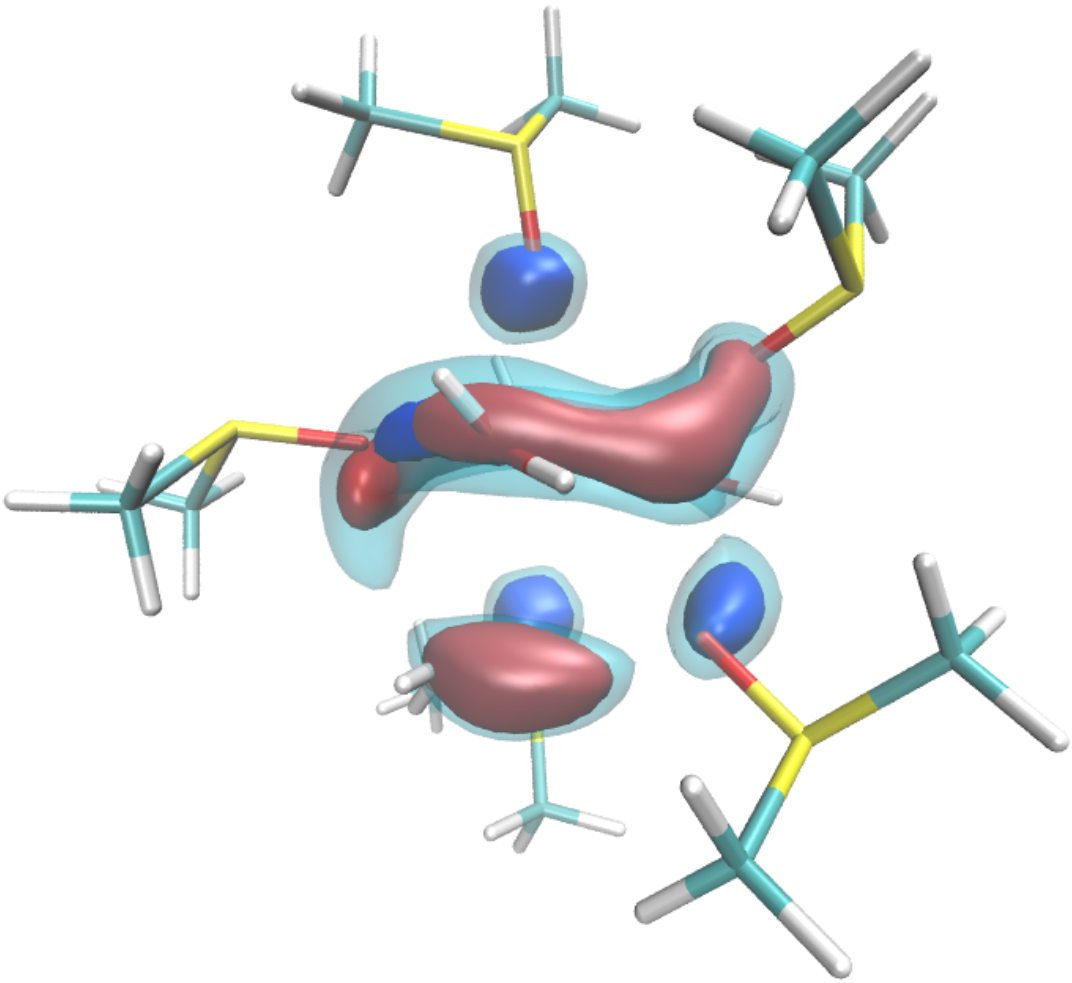

Figure 5: Spatial density distribution for the oxygen atoms in the first shell of the $Th^{4+}(H_2O)_4(DMSO)_5$ ion. Total density of oxygen atoms in transparent cyan color (the isosurface contains 5% of the total oxygen density). Water oxygen in red and DMSO oxygen in blue (both isosurfaces contains 10% of their respective total density).

above we have plotted the O-Th distances for water (left) and for DMSO (right) in the mixed, 1:1 solution. In the bottom panels we have reported the pure water (left) and pure DMSO (right) situations. As we can see from the pure solvent data (bottom panels), the water mobility in the first shell is much greater than that of DMSO. In the water solution we can trace many exchanges while no exchange is seen for DMSO. This is a result of (i) the stronger dipole of the DMSO molecule that makes the interaction with the ion more favorable, (ii) its larger mass that makes its diffusion slower and, finally, (iii) its larger steric volume which makes the exchange between the first and second shell much more difficult. In addition, inter-shell water molecule exchanges correspond to pairs of mutually exchanging water molecules and are promoted by H-bonding between the first and second shell[9] a feature which is missing in DMSO.

If we now look at data when mixing water and DMSO (top panels), we see that the situation has changed in the mixed solution: in particular the many exchanges of water molecules have disappeared and we clearly see the growth of a second shell of DMSO molecules that is forming by substitution of water molecules and that completes at 4 ns (see also Figure 4). This dynamical configuration is due again to the different characteristics of the two solvents. During the analyzed time in Figure 6, we see a progressive dehydration of the second shell of solvation in favor of DMSO. The latter, in fact, owing to its greater dipole moment, while it is unable to remove the tightly bound water molecules from the first shell, progressively substitutes the water molecules of the second shell. When the second shell is crowded of DMSO molecules (last 6 ns in the top panels of Figure 6) the water in first shell is no more surrounded by other water molecules and has no chance to leave the (first) shell. This is plausible since inter-shell water exchanges are promoted by the water-water interaction that is based on H-bonds.[9] In other words, the formation of this second shell of DMSO molecules segregates the water molecules in first shell from the other ones and makes impossible for water to form H-bonds with the surrounding molecules and prevents them from undergoing the dynamical exchanges that we have seen in the pure water simulation.

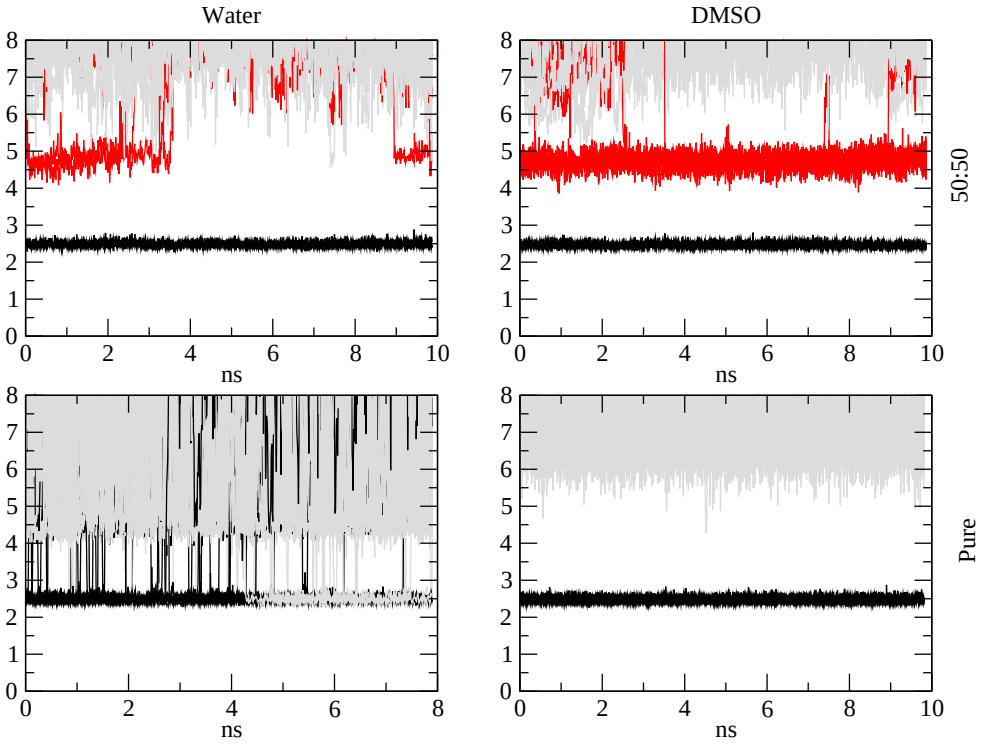

Figure 6: Th-O distance as a function of time. See text for details. For pure solvents (lower panels) Initially all the first shell ligands are reported in black and the others in gray. The color code black/gray has been chosen in order to highlight the exchanges. For the 1:1 solvation (upper panels) the color are set through the following convention: first shell molecules are in black, second shell ones are in red and gray is used for all others.

Conclusions

We have explored the solvation of Th^{4+} in three different liquids: water, DMSO and an equimolecular mixture of them. In order to study the structure and the dynamics of the solvent environment around the highly charged central ion, we have tailored a polarizable force filed within the Amoeba framework and used it in molecular dynamics simulation of the liquid phase. The use of a polarizable force field is mandatory given the highly energetic polarization phenomena that take place in the immediate surrounding of the ion. The force field van der Waals parameters for the Th^{4+} ion have been obtained from an adaptation procedure which is based on the comparison of the minimum geometries and energies of the $[Th(DMSO)_{8,9}]^{4+}$ clusters obtained with the force field with those obtained from rigorous ab-initio methods. The simulations in pure water and pure DMSO have provided a picture of the local nanoscopic solvation structure which is in agreement with the most recent experimental and simulation results, showing that the force field is transferable, making us confident in using it to mix the two solvents. The average coordination number of first shell ligands is near 9 for both pure solvents and the average oxygen-ion distance is 2.46 Å for water and 2.45 Å for DMSO. While, the structure with 10 first shell ligands appears to be a possible, albeit only slightly populated, geometric configuration in water, in DMSO, owing to its steric hindrance, the system seems unable to accommodate the tenth molecule in the first shell. When Th^{4+} is solvated by a 1:1 water:DMSO mixture, the first shell is still made by 9 molecules and composed by both solvents although the number of coordinated DMSO molecules (5) seems to be slightly larger than water (4). The average oxygen-ion distances remain similar to those detected in the pure solvation cases: 2.46 Å for water and 2.45 Å for DMSO. In conclusion, we can say that in an equimolecular mixture of water and DMSO, we have not found hints of a preferential solvation for Th^{4+}. What we have seen, however is the formation of a well structured situation that presents 9 ligands in the first shell, roughly half of which are water molecules that partake to the first solvation shell. The DMSO molecules, in addition to partially solvate directly the ion, arrange themselves in a

second shell of solvation that contains 8 molecules and no water.

Acknowledgement

Financial support of the Scientific Committee of the University of Rome through grant "Ricerca 2015" and of ANR 2010 JCJC 080701 ACLASOLV (Actinoids and Lanthanoids Solvation) are acknowledged. The support through grants IsC36_POLIL and IsC29_AAAIL of the CINECA supercomputing center and GENCI (grant x20131870 and x20141870) are also acknowledged.

Supporting Information Available

Force Field details and parameters. Th-ligand vibrational properties for force field validation. Mean square displacements vs time.

References

(1) Mathur, J. N.; Murali, M. S.; Nash, K. L. Actinide Partitioning – A Review. *Solvent Extr. Ion Exch.* **2001**, *19*, 357–390.

(2) Purroy, D.; Baron, P.; Christiansen, B.; Glatz, J. P.; Madic, C.; Malmbeck, R.; Modolo, G. First Demonstration of a Centrifugal Solvent Extraction Process for Minor Actinides From a Concentrated Spent Fuel Solution. *Sep. Purif. Technol.* **2005**, *45*, 157–162.

(3) Sui, N.; Huang, K.; Zhang, C.; Wang, N.; Wang, F.; Liu, H. Light, Middle, and Heavy Rare-Earth Group Separation: A New Approach via a Liquid-Liquid-Liquid Three-Phase System. *Ind. Eng. Chem. Res.* **2013**, *52*, 5997–6008.

(4) Radhika, S.; Kumar, B. N.; Kantam, M. L.; Reddy, B. R. Liquid-liquid Extraction and Separation Possibilities of Heavy and Light Rare-Earths From Phosphoric Acid Solutions With Acidic Organophosphorus Reagents. *Sep. Purif. Technol.* **2010**, *75*, 295–302.

(5) Banda, R.; Jeon, H.; Lee, M. Solvent Extraction Separation of Pr and Nd From Chloride Solution Containing La Using Cyanex 272 and Its Mixture With Other Extractants. *Sep. Purif. Technol.* **2012**, *98*, 481–487.

(6) Danilo Fontana, L. P. Separation of Middle Rare Earth by Solvent Extraction Using 2-ethylhexylphosphonic Acid Mono-2-ethylhexyl Ester as an Extraction. *J. Rare Earths* **2009**, *27*, 830–833.

(7) D'Angelo, P.; Spezia, R. Hydration of Lanthanoids(III) and Actinoids(III): An Experimental/Theoretical Saga. *Chem. Eur. J.* **2012**, *18*, 11162–11178.

(8) Moll, H.; Denecke, M. A.; Jalilehvand, F.; Sandstrom, M.; Grenthe, I. Structure of

the Aqua Ions and Fluoride Complexes of Uranium(IV) and Thorium(IV) in Aqueous Solution an EXAFS Study. *Inorg. Chem.* **1999**, *38*, 1795–1799.

(9) Yang, T.; Tsushima, S.; Susuki, A. Quantum Mechanical and Molecular Dynamical Simulations on Thorium(IV) Hydrates in Aqueous Solution. *J. Phys. Chem. A* **2001**, *105*, 10439–10445.

(10) Hagberg, D.; E.Bednarz,; N.M.Edelstein,; Gagliardi, L. A Quantum Chemical and Molecular Dynamics Study of the Coordination of Cm(III) in Water. *J. Am. Chem. Soc.* **2007**, *129*, 14136–14137.

(11) Skanthakumar, S.; Antonio, M.; Wilson, R.; Soderholm, L. The Curium Aqua Ion. *Inorg. Chem.* **2007**, *46*, 3285–3491.

(12) Tsushima, S. Hydrolysis and Dimerization of Th^{4+} Ion. *J. Phys. Chem. B* **2008**, *112*, 7080–7085.

(13) Brendebach, B.; Banik, N. L.; Marquardt, C. M.; Rothe, J.; Denecke, M.; Geckeis, H. X-ray Absorption Spectroscopic Study of Trivalent and Tetravalent Actinides in Solution at Varying pH Values. *Radiochim. Acta* **2009**, *97*, 701–7008.

(14) Frick, R. J.; Pribil, A. B.; Hofer, T. S.; Randolf, B. R.; Bhattacharjee, A.; Rode, B. M. Structure and Dynamics of the U^{4+} Ion in Aqueous Solution: An ab Initio Quantum Mechanical Charge Field Molecular Dynamics Study. *Inorg. Chem.* **2009**, *48*, 3993–4002.

(15) Galbis, E.; Hernandez-Cobos, J.; Den Auwer, C.; Naour, C. L.; Guillaumont, D.; Simoni, E.; Pappalardo, R. R.; Sanchez-Marcos, E. Solving the Hydration Structure of the Heaviest Actinide Aqua Ion Known: The Californium(III) Case. *Angew. Chem. Int. Ed.* **2010**, *49*, 3811–3815.

(16) R. E. Wilson, P. C. B., S. Skanthakumar; Soderholm, L. Structure of the Homoleptic Thorium(IV) Aqua Ion $[Th(H_2O)_{10}]Br_4$. *Angew. Chem., Int. Ed.* **2007**, *46*, 8043–8045.

(17) Wiebke, J.; Moritz, A.; Cao, X.; M.Dolg, Approaching Actinide(+III) Hydration From First Principles. *Phys. Chem. Chem. Phys.* **2007**, *9*, 459–465.

(18) Torapava, N.; Persson, I.; Eriksson, L.; Lundberg, D. Hydration and Hydrolysis of Thorium(IV) in Aqueous Solution and the Structures of Two Crystalline Thorium(IV) Hydrates. *Inorg. Chem.* **2009**, *48*, 11712–11723.

(19) Real, F.; Trumm, M.; Vallet, V.; Schimmelpfennig, B.; Masella, M.; Flament, J.-P. Quantum Chemical and Molecular Dynamics Study of the Coordination of Th(IV) in Aqueous Solvent. *J. Phys. Chem. B* **2010**, *114*, 15913–15924.

(20) Danilo, C.; Vallet, V.; Flament, J.-P.; Wahlgren, U. Effects of the First Hydration Sphere and the Bulk Solvent on the Spectra of the f^2 Isoelectronic Actinide Compounds: U_4^+, NpO_2^+, and PuO_2^{2+}. *Phys. Chem. Chem. Phys.* **2010**, *12*, 1116–1130.

(21) M. Duvail, P. V., F. Martelli; Spezia, R. Polarizable Interaction Potential for Molecular Dynamics Simulations of Actinoids(III) in Liquid Water. *J. Chem. Phys.* **2011**, *135*, 044503.

(22) Spezia, R.; Beuchat, C.; Vuilleumier, R.; D'Angelo, P.; Gagliardi, L. Unravelling Hydration Structure of Th(IV) and ThX_4 Water Solutions (X=Br, Cl) by Coupling Molecular Dynamics Simulations and X-ray Absorption Spectroscopy. *J. Phys. Chem. B* **2012**, *116*, 6465–6475.

(23) Marjolin, A.; Gourlaouen, C.; Clavaguera, C.; Ren, P. Y.; Wu, J. C.; Gresh, N.; Dognon, J.-P.; Piquemal, J.-P. Toward Accurate Solvation Dynamics of Lanthanides and Actinides in Water Using Polarizable Force Fields: From Gas-phase Energetics to Hydration Free Energies. *Theor. Chem. Acc.* **2012**, *131*, 11098.

(24) Leung, K.; Nenoff, T. M. Hydration Structures of U(III) and U(IV) Ions From Ab Initio Molecular Dynamics Simulations. *J. Chem. Phys.* **2012**, *137*, 074502.

(25) Atta-Fynn, R.; Johnson, D. F.; Bylaska, E. J.; Ilton, E. S.; Schenter, G. K.; de Jong, W. A. Structure and Hydrolysis of the U(IV), U(V), and U(VI) Aqua Ions from Ab Initio Molecular Simulations. *Inorg. Chem.* **2012**, *51*, 3016–3024.

(26) Real, F.; Trumm, M.; Schimmelpfennig, B.; Masella, M.; Vallet, V. Further Insights in the Ability of Classical Nonadditive Potentials to Model Actinide Ion–water Interactions. *J. Comput. Chem.* **2013**, *34*, 707–719.

(27) D'Angelo, P.; Martelli, F.; Spezia, R.; Filipponi, A.; Denecke, M. A. Hydration Properties and Ionic Radii of Actinide(III) Ions in Aqueous Solution. *Inorg. Chem.* **2013**, *52*, 10318–10324.

(28) Canaval, L. R.; Weiss, A. K.; Rode, B. M. Structure and Dynamics of the Th4+-ion in Aqueous Solution – An Ab Initio QMCF-MD Study. *Comput. Theo. Chem.* **2013**, *1022*, 94–102.

(29) Atta-Fynn, R.; Bylaska, E. J.; de Jong, W. A. Importance of Counteranions on the Hydration Structure of the Curium Ion. *J. Phys. Chem. Lett.* **2013**, *4*, 2166–2170.

(30) Spezia, R.; Jeanvoine, Y.; Beuchat, C.; Gagliardi, L.; Vuilleumier, R. Hydration Properties of Cm(III) and Th(IV) Combining Coordination Free Energy Profiles With Electronic Structure Analysis. *Phys. Chem. Chem. Phys.* **2014**, *16*, 5824–5832.

(31) Galbis, E.; Hernández-Cobos, J.; Pappalardo, R. R.; Marcos, E. S. Collecting High-order Interactions in an Effective Pairwise Intermolecular Potential Using the Hydrated Ion Concept: The Hydration of Cf_3^+. *J. Chem. Phys.* **2014**, 214104.

(32) Heinz, N.; Zhang, J.; Dolg, M. Actinoid(III) Hydration—First Principle Gibbs Energies

of Hydration Using High Level Correlation Methods. *J. Chem. Theory Comput.* **2014**, *10*, 5593–5598.

(33) Banik, N. l.; Vallet, V.; Real, F.; Belmecheri, R. M.; Schimmelpfennig, B.; Rothe, J.; Marsac, R.; Lindqvist-Reis, P.; Walther, C.; Denecke, M. A.; Marquardt, C. M. First Structural Characterization of Pa(IV) in Aqueous Solution and Quantum Chemical Investigations of the Tetravalent Actinides up to Bk(IV): the Evidence of a Curium Break. *Dalton Trans.* **2015**, –.

(34) Amador, D. H. T.; Sambrano, J. R.; Gargano, R.; de Macedo, L. G. M. Computational Study of Th^{4+} and Np^{4+} Hydration and Hydrolysis of Th4+ from First Principles. *J. Mol. Model.* **2017**, *23*, 69.

(35) Torapava, N.; Lundberg, D.; Persson, I. A Coordination Chemistry Study of Solvated Thorium(IV) Ions in Two Oxygen-Donor Solvents. *Eur. J. Inorg. Chem* **2011**, *2011*, 5273–5278.

(36) Soga, T. The Resonance Raman Effect of Uranyl Formate in Dimethyl Sulfoxide. *Spectrochim. Acta A Mol. Biomol. Spectrosc.* **2003**, *59*, 2497–2510.

(37) Bernardo, P. D.; Zanonato, P. L.; Benetollo, F.; Melchior, A.; Tolazzi, M.; Rao, L. Energetics and Structure of Uranium(VI)–Acetate Complexes in Dimethyl Sulfoxide. *Inorganic Chemistry* **2012**, *51*, 9045–9055.

(38) Takao, K.; Takao, S.; Ikeda, Y.; Bernhard, G.; Hennig, C. Uranyl-halide Complexation in N,N-dimethylformamide: Halide Coordination Trend Manifests Hardness of $[UO_2]^{2+}$. *Dalton Trans.* **2013**, *42*, 13101–13111.

(39) Weis, E. M.; Duval, P. B.; Jurisson, S. S. Syntheses and Structures of Two Uranyl Complexes With DMPU. *Radiochim. Acta* **2012**, *100*, 237–241.

(40) Day, V. W.; Hoard, J. L. Stereochemistry of Tropolonato Complexes Utilizing the Higher Coordination Numbers. I. Nine-coordinate Tetrakis(tropolonato)-N,N'-dimethylformamidethorium(IV). *J. Am. Chem. Soc.* **1970**, *92*, 3626–3635.

(41) Bonfada, E.; Schulz-Lang, E.; Zan, R. A.; Abram, U. Z. Syntheses and Structures of Thorium(IV) Complexes with Bis(diphenylphosphino)ethane Dioxide, $Ph_2P(O)CH_2CH_2P(O)Ph_2$, and Bis(diphenylphosphoryl)amide, $[Ph_2P(O)NP(O)Ph_2]^-$. *Naturforsch. Ser. B* **2000**, *55*, 285–290.

(42) Carvalho, A.; Garcia-Montalvo, V.; Domingos, A.; Cea-Olivares, R. Synthesis and Characterization of Thorium and Uranium Tetraphenylimidophosphinate complexes. Crystal and Molecular Structures of $Th(tpip)_4$, $U(tpip)_4$ and $UCl(tpip)_3$. *Polyhedron* **2000**, *19*, 1699–1705.

(43) Berthet, J. C.; Nierlich, M.; Ephritikhine, M. Synthesis of Organouranium(IV) Triflates From U(OTf)4 or From Alkyl or Amide Precursors. *Eur. J. Inorg. Chem.* **2002**, 850–858.

(44) Berthet, J. C.; Thuery, P.; Ephritikhine, M. New Efficient Synthesis of $[UI_4(MeCN)_4]$. X-ray Crystal Structures of $[UI_2(MeCN)_7][UI_6]$, $[UI_4(py)_3]$, and $[U(dmf)_9]I_4$. *Inorg. Chem.* **2005**, *44*, 1142–1146.

(45) Harrowfield, J. M.; Ogden, M. I.; Skelton, B. W.; White, A. H. Actinide Coordination Chemistry – a Unique Example of a Homoleptic Complex of Nine-Coordinate Thorium(IV). *Inorg. Chim. Acta* **2004**, *357*, 2404–2406.

(46) Kaltsoyannis, N.; Scott, P. *The f elements*; Oxford Chemistry Primers; Oxford University Press, Oxford, 2007.

(47) Montagna, M.; Jeanvoine, Y.; Spezia, R.; Bodo, E. Structure, Stability, and Electronic Properties of Dimethyl Sulfoxide and Dimethyl Formammide Clusters Containing Th^{4+}. *J. Phys. Chem. A* **2016**, *120*, 4778–4788.

(48) Bodo, E.; Chiricotto, M.; Spezia, R. Structural, Energetic and Electronic Properties of La(III)-DMSO Clusters. *J. Phys. Chem. A* **2014**, *118*, 11602–11611.

(49) Ponder, J. W.; Wu, C.; Ren, P.; Pande, V. S.; Chodera, J. D.; Schnieders, M. J.; Haque, I.; Mobley, D. L.; Lambrecht, D. S.; DiStasio, R. A.; Head-Gordon, M.; Clark, G. N. I.; Johnson, M. E.; Head-Gordon, T. Current Status of the AMOEBA Polarizable Force Field. *J. Phys. Chem. B* **2010**, *114*, 2549–2564, PMID: 20136072.

(50) TINKER - Software Tools for Molecular Design, dasher.wustl.edu/tinker/.

(51) Bodo, E.; Macaluso, V.; Spezia, R. Solvent Structure Around Lanthanoids(III) Ions in Liquid DMSO as Revealed by Polarizable Molecular Dynamics Simulations. *J. Phys. Chem. B* **2015**, 13347–13357.

(52) Real, F.; Vallet, V.; Clavaguera, C.; Dognon, J.-P. In silico prediction of atomic static electric-dipole polarizabilities of the early tetravalent actinide ions: Th^{4+} $(5f^0)$, $Pa^{4+}(5f^1)$, and U^{4+} $(5f^2)$. *Phys. Rev. A* **2008**, *78*, 052502.

(53) Dolg, M.; Stoll, H.; Preuss, H.; Pitzer, R. M. Relativistic and Correlation Effects for Element 105 (Hahnium, Ha): a Comparative Study of M and MO (M = Nb, Ta, Ha) Using Energy-Adjusted Ab Initio Pseudopotentials. *J. Phys. Chem.* **1993**, *97*, 5852–5859.

(54) Berendsen, H. J. C.; Postma, J. P. M.; van Gunsteren, W. F.; Di Nola, A.; Haak, J. R. Molecular Dynamics with Coupling to an External Bath. *J. Chem. Phys.* **1984**, *81*, 3684–3690.

(55) LeBel, R. G.; Goring, D. A. I. Density, Viscosity, Refractive Index, and Hygroscopicity of Mixtures of Water and Dimethyl Sulfoxide. *J. Chem. Eng. Data* **1962**, *7*.

(56) Sato, H.; Yui, M.; Yoshikawa, H. Ionic Diffusion Coefficients of Cs^+, Pb^{2+}, Sm^{3+}, Ni^{2+},

SeO_4^{2-} and TcO_4^- in Free Water Determined from Conductivity Measurements. *J. Nucl. Sc. Tech.* **1996**, *33*.

(57) Duvail, M.; Souaille, M.; Spezia, R.; Cartailler, T.; Vitorge, P. Pair Interaction Potentials With Explicit Polarization for Molecular Dynamics Simulations of La^{3+} in Bulk Water. *J. Chem. Phys.* **2007**, *127*, 034503.

(58) Duvail, M.; Vitorge, P.; Spezia, R. Building a Polarizable Pair Interaction Potential for Lanthanoids(III) in Liquid Water : a Molecular Dynamics Study of Structure and Dynamics of the Whole Series. *J. Chem. Phys.* **2009**, *130*, 104501.

(59) Atta-Fynn, R.; Bylaska, E. J.; de Jong, W. A. Strengthening of the Coordination Shell by Counter Ions in Aqueous Th^{4+} Solutions. *J. Phys. Chem. A* **2016**, *120*.

(60) D'Angelo, P.; Zitolo, A.; Migliorati, V.; Chillemi, G.; Duvail, M.; Vitorge, P.; Abadie, S.; Spezia, R. Revised Ionic Radii of Lanthanoid(III) Ions in Aqueous Solution. *Inorg. Chem.* **2011**, *50*, 4572–4579.

(61) Helm, L.; Merbach, A. E. Inorganic and Bioinorganic Solvent Exchange Mechanisms. *Chem. Rev.* **2005**, *105*, 1923–1960.

For Table of Contents Only

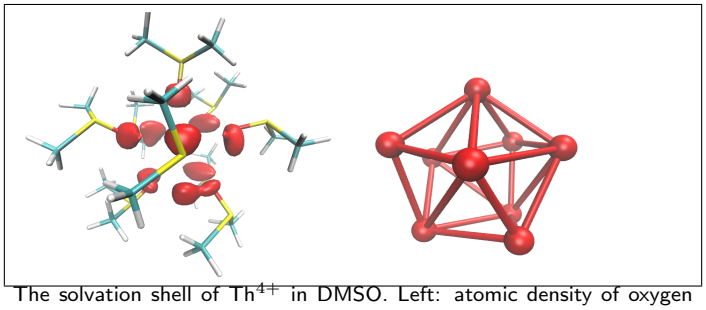

The solvation shell of Th^{4+} in DMSO. Left: atomic density of oxygen atoms as obtained from polarizable MD. Right: "ball-and-stick" representation of the first cordination shell.